Microelectronics Reliability xxx (2017) xxx–xxx

Contents lists available at ScienceDirect

Microelectronics Reliability

journal homepage: www.elsevier.com/locate/microrel

Identification of the generation/rupture mechanism of filamentary conductive paths in ReRAM devices using oxide failure analysis

A. Rodriguez-Fernandez [a,*], C. Cagli [b], L. Perniola [b], J. Suñé [a], E. Miranda [a]

[a] Departament d'Enginyeria Electrònica, Universitat Autònoma de Barcelona, Cerdanyola del Vallès, Spain
[b] CEA, LETI, MINATEC Campus, Grenoble, France

ARTICLE INFO

Article history:
Received 19 May 2017
Received in revised form 26 June 2017
Accepted 30 June 2017
Available online xxxx

Keywords:
MIM
ReRAM
Breakdown
Reliability

ABSTRACT

Constant (CVS) and ramped (RVS) voltage stress data are combined with the aim of identifying the acceleration law that drives the generation and rupture of filamentary conductive paths in HfO_2-based ReRAM devices. The acceleration factor integral (AFI) method is used to find the equivalency between RVS and CVS in order to compare the SET and RESET events statistics and determine the adequacy of different degradation models frequently considered in oxide failure analysis: voltage power-law, *E*-model, and 1/*E*-model. The obtained results indicate that the *E*-model, with *E* the local electric field, exhibits the lowest dispersion in the acceleration factor values both for the SET and RESET transitions as well as the best overall consistency.

1. Introduction

Understanding the generation and rupture mechanisms of filamentary conductive paths in thin oxide films is of utmost importance for the application of these structures in resistive random access memories (ReRAM) [1]. This not only requires models able to describe the physics behind such events but also statistical tools appropriate for dealing with their intrinsic stochastic nature. The observed randomness is nothing but a consequence of cycle-to-cycle microscopic changes in these conductive paths. In this work, constant (CVS) and ramped (RVS) voltage stress data are conveniently combined with the purpose of identifying the most suitable acceleration law for the formation and rupture of conductive filaments (CF) in HfO_2-based ReRAM devices. The SET event is associated with the transition from the high (HRS) to the low resistance state (LRS), while the RESET event with the transition in the opposite direction. For the investigated devices, these events take place under opposite voltage polarities (bipolar switching). The models considered in this study are the power-law (V^{-n}) model, the *E*-model and the 1/*E*-model, where *V* and *E* are the applied voltage and the local electric field, respectively [2]. In order to compare CVS with RVS data for the SET and RESET events, the acceleration factor integral (AFI) method is considered [3–5]. This method allows assessing the adequacy of different degradation models and selecting the most reliable one in terms of overall consistency. Notice that these acceleration models are frequently applied to oxide layers which have not suffered a previous breakdown event, i.e. a forming process [6]. According to the obtained results, the *E*-model seems to be the best option, at least for the voltage range and ramp rates investigated here. The underlying physical picture for this model (also called thermochemical in oxide reliability analysis [7]) is consistent with current theories relating the formation and dissolution of CFs in ReRAMs with field and temperature-assisted atomic displacements [1]. Failure distributions are commonly used to identify the breakdown mechanism and calculate the acceleration parameters [8]. As it will be shown in this paper, similarly to what happens in oxide failure analysis, time-to-breakdown statistics using CVS in a narrow voltage window (set by practical limitations) does not yield conclusive results. In order to correctly identify the appropriate acceleration law, this information needs to be complemented with analysis arising from alternative approaches such as the AFI method for RVS. Ultimately, this kind identification can give further support or not to any of the proposed physical mechanism ascribed to the formation and dissolution of CFs.

2. Experimental details

The ReRAM cells investigated in this work were fabricated at LETI (CEA) and consist in 10 nm-thick atomic layer-deposited HfO_2 films sandwiched between Ti and TiN metal electrodes. The cell is connected in series with a NMOS transistor, embedding a one transistor-one resistor (1T1R) structure. The NMOS transistor is used to prevent irreversible cell breakdown by limiting the current in the RRAM low resistive state (LRS). An electroforming step with gate voltage $V_G = 1.3$ V is required to activate the switching property of the device. Quasi-static *I-V-t* measurements were performed using a Keithley 4200-SCS semiconductor parameter analyzer equipped with a 4225-RPM PGU (pulse generator

* Corresponding author.
E-mail address: alberto.rodriguez@uab.cat (A. Rodriguez-Fernandez).

http://dx.doi.org/10.1016/j.microrel.2017.06.088
0026-2714/

unit). Data were obtained using pulsed measurements ($\Delta V = 50$ mV) with pulse widths ranging from 1 μs to 1 ms corresponding to ramp rates (*RR*) in the range from 50 V s^{-1} to 50 KV s^{-1}. Fig. 1 shows typical bipolar resistive switching characteristics ($RR = 50$ V s^{-1}). The SET process exhibits a sharp transition. The current compliance level (I_C) is adjusted by setting $V_G = 1.3$ V. Instead, the RESET process is gradual. $V_G = 4$ V is used to avoid any current limitation during the transition. The corresponding I_C levels for both gate voltage conditions are 130 μA and 3.5 mA. The red solid line in Fig. 1 represents the median curve of 50 cycles. In what follows, all the *I-V* curves shown correspond to 50 cycles as well. Notice that V_{SET} and V_{RESET} are lower than 0.8 V, which suggests that the devices investigated here are suitable for low voltage applications [9]. Importantly, in the analysis performed, the voltage and not the electric field was used as the acceleration variable because the width of the insulating gap along the CF (when disrupted) does not necessarily coincide with the nominal oxide thickness.

3. Data analysis and discussion

To illustrate the effects of *RR* on the SET process, experimental *I-V* characteristics for different *RR* values are shown in Fig. 2.a. The RESET process is always performed with $RR = 50$ V s^{-1}. Clearly, V_{SET} increases as *RR* increases. Similar results are illustrated in Fig.2.b for the RESET process: V_{RESET} increases as *RR* increases. In this case, $RR = 50$ V s^{-1} is kept fixed for the SET process. In close agreement with the results reported in [10–15], V_{SET} and V_{RESET} follow the same logarithmic dependence with *RR*, which suggests that, beyond their particular features, the SET and RESET events share a common physical origin. The input signal (*V-t*) used to perform cycling at different *RR* are shown in the insets of Fig. 2. In addition, the SET time (t_{SET}) was determined using CVS. For the sake of clarity, the definitions used in this work for CVS and RVS are shown in Fig. 3. Fig. 4 illustrates a typical CVS experiment for the SET process (positive bias), from A to C with the corresponding RVS for the RESET process (negative bias), beginning at C and ending at A again. The experiment consists in 100 cycles performed per CVS at $V_{CVS} = 0.45$, 0.50, 0.55, 0.60, and 0.65 V. While the lower voltage limit is set by the measurement duration, the upper limit almost coincides with the sudden transition to LRS. Fig. 5.a shows Weibull plots for t_{SET} obtained by CVS. The associated Weibits can be expressed as:

$$\ln(-\ln(1-F)) = \beta \ln(t_{SET}/t_{63\%}) \quad (1)$$

where *F* is the cumulative distribution function, β the shape factor, and $t_{63\%}$ the scale factor. β values are in the range from 0.95 to 1.1 and increases with the applied voltage as it can be seen in Fig. 5.b and c.

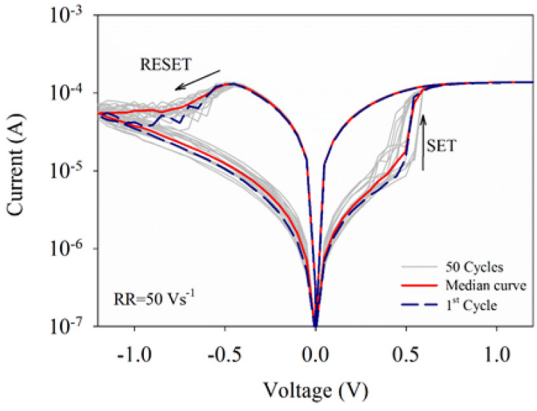

Fig. 1. Bipolar resistive switching behavior during successive set and reset cycles using quasi-static sweeps (RR = 50Vs^{-1}). First cycle (blue dashed line), 50 curves (grey solid lines) and its median (red heavy solid line) are shown. (For interpretation of the references to color in this figure legend, the reader is referred to the web version of this article.)

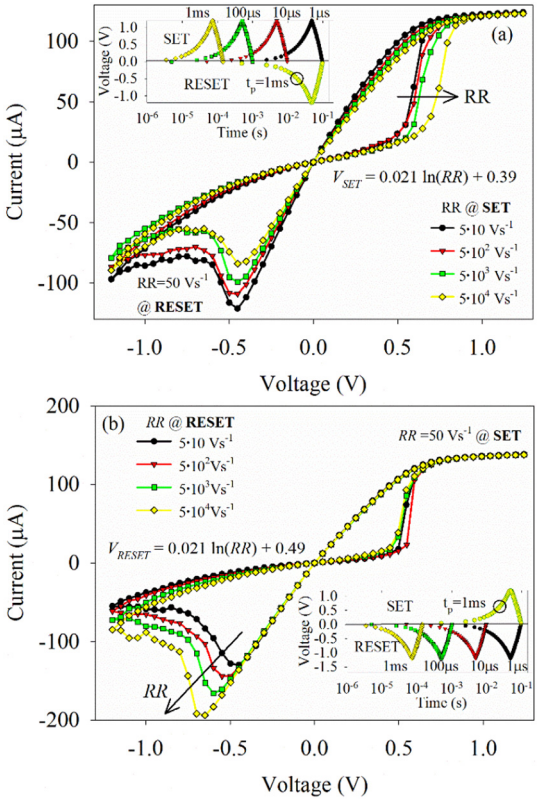

Fig. 2. Measured I-V characteristics for different RR values during: (a) set process and (b) reset process. The reset RR and the set RR are kept constant at 50 V s^{-1}, respectively. Insets show the input signal (V-t) used to perform cycling at different RR. Different width pulse times (t_p) ranging from 1 μs to 1 ms and a ramp step voltage of 50 mV are used.

Fig. 6 shows $t_{63\%}$ fitting results for the three voltage acceleration models under consideration. The *E*-model is expressed in terms of the applied voltage V_{CVS} as [16,17]:

$$E\text{-model}: \ \ln(t_{63\%}) = \ln(a) - \gamma V_{CVS} \quad (2)$$

where γ is the acceleration factor parameter and *a* a fitting constant. The power-law model reads:

$$\text{Power-law}: \ \ln(t_{63\%}) = b - n \cdot \ln(V_{CVS}) \quad (3)$$

where *b* is a fitting constant and *n* the acceleration factor. The 1/*E*-model is often assumed to be related to tunneling through the dielectric film and takes the form:

$$1/E\text{-model}: \ \ln(t_{63\%}) = c + \delta/V_{CVS} \quad (4)$$

where *c* is a fitting constant and δ the acceleration factor. Acceleration parameters $\gamma \sim 45.8$ V^{-1}, $n \sim 24.9$, and $\delta \sim 13.3$ V are found for the respective CVS fittings (see Table 1).

Fig. 7 shows the effects of *RR* on V_{SET}. Symbols are experimental data (50 cycles each point) and solid lines are guides to the eye corresponding to five different devices. Dotted, dashed, and dot-dashed lines correspond to simulated results obtained by the AFI method (see the Appendix). Briefly, the method consists in representing CVS data in terms of equivalent RVS data. Alternatively, it can be used to represent RVS data in terms of equivalent CVS. Although the simulated curves are in good agreement with the experimental data (see Fig. 7), deviations for the 1/*E*- and power-law models are detected at the highest *RR*s. On the contrary, the *E*-model follows a straight-line compatible with the whole set of observations. Reliable CVS data for the RESET transition is difficult to achieve since at the outset of the experiment the

Please cite this article as: A. Rodriguez-Fernandez, et al., Identification of the generation/rupture mechanism of filamentary conductive paths in ReRAM devices using oxide failure analysis, Microelectronics Reliability (2017), http://dx.doi.org/10.1016/j.microrel.2017.06.088